# Exosomal microRNA-448 suppresses the malignant behaviors of liver cancer cells by targeting RAB7A and inhibiting glycolysis

YUANKUN CHEN[1,2*], TIANTIAN ZHU[3*], FANG CHEN[1*], MINGYUE NIU[3], HAIFENG WU[1], QIUPING WU[1], ZHENG WANG[4] and WENTING LI[5]

[1]Department of Tropical and Liver Diseases, The Second Affiliated Hospital of Hainan Medical University, Haikou, Hainan 570100, P.R. China; [2]Department of Clinical Laboratory, The Second Affiliated Hospital of Hainan Medical University, Haikou, Hainan 570311, P.R. China; [3]Department of Emergency Medicine, The First Affiliated Hospital of Anhui Medical University, Hefei, Anhui 230022, P.R. China; [4]Department of Respiratory and Critical Medicine, People's Hospital of Zhengzhou University, Zhengzhou, Henan 450003, P.R. China; [5]Department of Infectious Diseases, The First Affiliated Hospital of Anhui Medical University, Hefei, Anhui 230022, P.R. China

Received April 30, 2025; Accepted November 24, 2025

DOI: 10.3892/ol.2026.15450

**Abstract.** Liver cancer is a highly aggressive cancer and the regulatory roles of microRNAs (miRs) in its progression are still being explored. miR-448, which is implicated in several types of cancer, remains to be fully characterized in liver cancer, particularly regarding its presence in exosomes. The aim of the present study was to examine the effects of exosomal miR-448 (EXO-miR-448) on liver cancer cell behavior. The expression levels of miR-448 in human liver cancer cell lines and its localization in exosomes were analyzed using reverse transcription-quantitative PCR, transmission electron microscopy and nanoparticle tracking analysis, with western blotting performed to detect exosomal markers. Functional assays were conducted to assess the effects of EXO-miR-448 on cell proliferation, migration and invasion. The results demonstrated that miR-448 expression was significantly downregulated in human liver cancer cell lines (HepG2, Hep3B and SK-HEP-1) compared with that in normal liver cells. Furthermore, exosomal analysis confirmed that miR-448 was enriched within exosomes rather than being secreted into the supernatant. EXO-miR-448 also inhibited liver cancer cell proliferation, migration and invasion, as demonstrated using Cell Counting Kit-8 and Transwell assays. Bioinformatics and functional assays further identified Ras-related protein Rab-7a (RAB7A) as a direct downstream target of miR-448, with its overexpression rescuing the inhibitory effects of EXO-miR-448 on cell behavior. Furthermore, EXO-miR-448 suppressed glycolysis in liver cancer cells by targeting RAB7A, as indicated by reduced lactate production, glucose uptake, ATP levels and extracellular acidification rate. In conclusion, EXO-miR-448 inhibits liver cancer cell proliferation, migration, invasion and glycolysis by targeting RAB7A. These findings underscore the importance of miR-448 in liver cancer biology and support its further evaluation in future translational studies.

*Correspondence to:* Professor Wenting Li, Department of Infectious Diseases, The First Affiliated Hospital of Anhui Medical University, 218 Jixi Road, Shushan, Hefei, Anhui 230022, P.R. China
E-mail: wtl9911002ah@163.com

Professor Zheng Wang, Department of Respiratory and Critical Medicine, People's Hospital of Zhengzhou University, 7 Weiwu Road, Jinshui, Zhengzhou, Henan 450003, P.R. China
E-mail: santawang99@163.com

*Contributed equally

*Key words:* microRNA-448, Ras-related protein Rab-7a, liver cancer, glycolysis, exosomes

## Introduction

Liver cancer remains one of the leading causes of cancer-related mortality globally (865,269 new cases and 757,948 deaths in 2022), with a high incidence in regions affected by chronic liver diseases such as hepatitis B and C infection (1-3). Despite advances in early detection and treatment strategies, the prognosis for patients with liver cancer remains poor, mainly due to the aggressive nature of the tumor, including its ability to metastasize and develop resistance to conventional therapies, such as surgical resection, ablation therapy and transarterial chemoembolization (4). Therefore, there is a key need to identify novel biomarkers and mechanistic regulators of liver cancer that may inform future therapeutic development.

MicroRNAs (miRNAs/miRs) are small non-coding RNAs that post-transcriptionally regulate gene expression and are involved in several biological processes, including cell proliferation, differentiation, apoptosis and metabolism (5,6). In cancer, miRNAs can function as either oncogenes or tumor suppressors, depending on their target genes and the cellular context (7). miR-448 has been identified as a tumor suppressor in several types of cancer, including breast, gastric and liver cancer, where it is implicated in the regulation of cell proliferation, migration and invasion (8-11). However, the precise molecular mechanisms underlying its role in liver cancer progression remain to be elucidated.

One of the hallmarks of cancer cells is altered metabolism, with a particular emphasis on the reprogramming of glucose metabolism. The Warburg effect, characterized by the upregulation of glycolysis even in the presence of oxygen, is a common metabolic shift observed in several types of cancer, including liver cancer, ovarian cancer, colorectal cancer and non-small cell lung cancer (12-15). This metabolic alteration supports the high energy demands of rapidly proliferating cancer cells, and facilitates tumor progression and metastasis (16). Previous studies have suggested that miRNAs, including miR-448, miR-126-3p and miR-423-5p, may modulate glycolysis as well as lipid and amino acid metabolism, although the direct association between miR-448 and glycolytic regulation in liver cancer remains to be elucidated (17-19).

Ras-related protein Rab-7a (RAB7A), a member of the small GTPase family, serves a key role in vesicular trafficking and endosomal maturation. It has been reported to regulate numerous cellular processes, including autophagy, metabolism and cell migration (20). Furthermore, RAB7A has been shown to be upregulated in several types of cancer, including hepatocellular carcinoma (HCC), pancreatic adenocarcinoma and colon adenocarcinoma, and its elevated expression is associated with poor prognosis and aggressive tumor behavior (21-23). Recent studies have suggested that RAB7A may influence glycolytic metabolism in cancer cells, although its role in liver cancer glycolysis is yet to be fully elucidated (24,25).

It was hypothesized in the present study that exosomal miR-448 (EXO-miR-448) suppresses liver cancer progression by directly targeting RAB7A and inhibiting glycolytic metabolism. Therefore, the current study aimed to assess the expression levels of RAB7A and miR-448 in liver cancer and normal liver cell lines, to explore the relationship between EXO-miR-448 and RAB7A, and to evaluate the effects of EXO-miR-448 on proliferation, migration, invasion and glycolytic activity in liver cancer cells.

## Materials and methods

*Cell lines and culture conditions*. All cell lines (HepG2, Hep3B, SK-HEP-1 and THLE-2) were purchased from the American Type Culture Collection. The identity of all cell lines was confirmed by the supplier using short tandem repeat profiling. In addition, all cell lines were routinely cultured for <10 passages and tested negative for mycoplasma contamination using PCR-based assays prior to use. Cells were maintained at 37˚C in a humidified atmosphere containing 5% $CO_2$ using DMEM (Gibco; Thermo Fisher Scientific, Inc.) supplemented with 10% FBS (Gibco; Thermo Fisher Scientific, Inc.) and 1% penicillin-streptomycin solution. The use of commercially obtained human cell lines was approved by the Ethics Committee of The Second Affiliated Hospital of Hainan Medical University (Haikou, China) and all procedures were performed in accordance with institutional guidelines.

*Exosome isolation and identification*. Exosomes were isolated from HepG2 cell culture supernatants using ultracentrifugation. Briefly, the cell culture supernatant was sequentially centrifuged at 300 x g for 10 min at 4˚C, 2,000 x g for 10 min at 4˚C and 10,000 x g for 30 min at 4˚C to remove cells and debris, followed by ultracentrifugation at 100,000 x g for 70 min at 4˚C to pellet exosomes. Exosomes were identified by transmission electron microscopy (TEM; JEOL, Ltd.), nanoparticle tracking analysis (NTA; ZetaView®; Particle Metrix GmbH), and western blotting of exosomal markers and a negative control (CD63: 1:500, cat. no. ab68418, Abcam; CD9: 1:500, cat. no. WL06408, Wanleibio Co., Ltd.; calnexin:1:500, cat. no. WL03062, Wanleibio Co., Ltd.). For TEM analysis, isolated exosomes were examined without fixation, embedding or sectioning. A 10 $\mu$l exosome suspension was placed onto a carbon-coated copper grid and allowed to adsorb for 10 min at 25˚C. Excess liquid was removed with filter paper, followed by negative staining with 2% phosphotungstic acid for 2 min at 25˚C. The grids were then air dried and examined using TEM. For NTA, the sample chamber was first rinsed with deionized water, and the instrument was calibrated using 110 nm polystyrene microspheres. The chamber was then washed with PBS, and exosome samples were diluted 1:200 in PBS before measurement using the ZetaView instrument.

*RNA extraction and reverse transcription-quantitative PCR (RT-qPCR)*. Total RNA was extracted from cultured cells (THLE-2, SK-HEP-1, Hep3B and HepG2) or isolated exosomes using TRIzol® reagent (Invitrogen; Thermo Fisher Scientific, Inc.) according to the manufacturer's instructions. For mRNA analysis, RNA was reverse-transcribed into cDNA using a PrimeScript™ RT reagent kit (Takara Bio, Inc.), whereas for miRNA analysis, cDNA was synthesized using a miRNA First-Strand cDNA Synthesis Kit (Tailing Reaction) (cat. no. B532451; Sangon Biotech Co., Ltd.), according to the manufacturers' protocols. Subsequently, qPCR was performed on a 7500 Real-Time PCR System (Applied Biosystems; Thermo Fisher Scientific, Inc.). miRNA expression was analyzed using 2X Fast Taq Plus PCR Master Mix (Biosharp Life Sciences) supplemented with SYBR Green (Beijing Solarbio Science & Technology Co., Ltd.) under the following conditions: 95˚C for 10 min, followed by 40 cycles at 95˚C for 20 sec, 60˚C for 20 sec and 70˚C for 10 sec, with melting curve analysis performed at the end of amplification. mRNA expression was analyzed using SYBR® Premix Ex Taq™ II (Takara Bio, Inc.) according to the manufacturer's protocol, with the following thermocycling conditions: Initial denaturation at 95˚C for 30 sec, followed by 40 cycles at 95˚C for 5 sec and 60˚C for 34 sec. The relative expression levels of miR-448 were normalized to U6, whereas those of RAB7A, sphingosine-1-phosphate phosphatase 1 (SGPP1), vasohibin 2 (VASH2), mitochondrial pyruvate carrier 1 (MPC1) and thymosin β 4 X-linked (TMSB4X) were normalized to β-actin using the $2^{-\Delta\Delta Cq}$ method (26). Primer sequences for mRNA targets and β-actin were synthesized by Sangon Biotech Co., Ltd. and are listed in Table I. The forward primer for hsa-miR-448 was synthesized by General Biotech (Anhui) Co., Ltd. The reverse primer for miR-448 and the U6 primer were supplied as built-in components of the miRNA First-Strand cDNA Synthesis Kit.

*RNase A and Triton X-100 treatment for verification of EXO-miR-448*. To determine whether miR-448 in the culture supernatant was encapsulated within exosomes, the conditioned medium of HepG2 cells was collected and centrifuged at 300 x g for 10 min and 2,000 x g for 10 min at 4˚C to remove cells and cellular debris. The supernatants were then treated

Table I. Primer sequences used for reverse transcription-quantitative PCR.

| Gene | Primer sequence, 5'-3' |
|---|---|
| RAB7A | F: GACTGCTGCGTTCTGGT |
| | R: CCTCCGTTTCCTGCTTA |
| β-actin | F: GGCACCCAGCACAATGAA |
| | R: TAGAAGCATTTGCGGTGG |
| hsa-miR-448 | F: TTGCATATGTAGGATGTCCCAT |
| SGPP1 | F: CTCCATTCATCATCATCGGGCTTC |
| | R: CTAGTATCTCGGCTGTGTCTCCTC |
| VASH2 | F: AGGAACGCCGCCTTCTTGG |
| | R: CATGTAATTCTGGATCGCCTGGAG |
| MPC1 | F: TGCCCTCTGTTGCTATTCTTTGAC |
| | R: AGCCGCCCTCCCTGGATG |
| TMSB4X | F: CTGACAAACCCGATATGGCTGAG |
| | R: GCCTGCTTGCTTCTCCTGTTC |

F, forward; miR, microRNA; MPC1, mitochondrial pyruvate carrier 1; SGPP1, sphingosine-1-phosphate phosphatase 1; R, reverse; RAB7A, Ras-related protein Rab-7a; TMSB4X, thymosin β 4 X-linked; VASH2, vasohibin 2.

with RNase A (100 $\mu$g/ml) at 37˚C for 60 min to degrade free extracellular miRNA, or with RNase A (100 $\mu$g/ml) plus Triton X-100 (1%) at 37˚C for 30 min to disrupt vesicle membranes and degrade encapsulated miRNA. Subsequently, the levels of miR-448 in the supernatants were determined by RT-qPCR using the aforementioned procedure.

*Preparation and verification of miR-448 enriched exosomes*. HepG2 cells were used as donor cells to generate miR-448 enriched exosomes. HepG2 cells were seeded in 6-well plates at a density of $2x10^5$ cells/well. Cells were transfected with miR-448 mimics or control mimics (mimics NC) (JTS Scientific Co., Ltd.) using Lipofectamine® 3000 (Invitrogen; Thermo Fisher Scientific, Inc.), with 75 pmol mimics/well in a final volume of 2.5 ml, and incubated at 37˚C for 48 h according to the manufacturer's instructions. The sequences were as follows: miR-448 mimics, sense 5'-UUGCAUAUG UAGGAUGUCCCAU-3', antisense 5'-GGGACAUCCUAC AUAUGCAAUU-3'; And mimics NC, sense 5'-UUCUCC GAACGUGUCACGUTT-3', antisense 5'-ACGUGACAC GUUCGGAGAATT-3'. After 48 h, the culture supernatant was collected and exosomes were isolated by differential ultracentrifugation (300 x g for 10 min, 2,000 x g for 10 min, 10,000 x g for 30 min and 100,000 x g for 70 min, all at 4˚C). Exosomes derived from miR-448 mimic-transfected donor cells and mimics NC-transfected donor cells were designated EXO-miR-448 and EXO-NC, respectively. For functional assays, HepG2 cells were treated with EXO-miR-448 or EXO-NC (25 $\mu$g/ml) at 37˚C. Cells were analyzed at 0, 24, 48 and 72 h for the Cell Counting Kit-8 (CCK-8) assay, whereas for EdU, migration and invasion assays, cells were analyzed after 48 h of exosome treatment. To confirm the successful enrichment of miR-448 in exosomes, total RNA was extracted from the isolated exosomes, and RT-qPCR was performed to quantify miR-448 expression levels.

*Western blot analysis*. Cells (THLE-2, SK-HEP-1, Hep3B and HepG2) or isolated exosomes were lysed using RIPA buffer (Beyotime Biotechnology) containing protease inhibitors and protein concentrations were determined using the BCA Protein Assay Kit (Thermo Fisher Scientific, Inc.). Equal amounts of protein samples (40 $\mu$g/lane) were separated by SDS-PAGE on a 5% stacking gel, and 8 or 13% separating gels, and transferred onto PVDF membranes (MilliporeSigma). Subsequently, the membranes were blocked with 5% skim milk at 37˚C for 2 h, and were incubated overnight at 4˚C with the following primary antibodies: RAB7A (1:1,000; cat. no. A12308; ABclonal Biotech Co., Ltd.), CD63, CD9, calnexin and β-actin (1:1,000; cat. no. WL01372; Wanleibio Co., Ltd.). The membranes were then incubated with an HRP-conjugated secondary antibody (goat anti-rabbit IgG-HRP; 1:5,000; cat. no. WLA023; Wanleibio Co., Ltd.) at 37˚C for 2 h. Protein bands were visualized using the Clarity™ Western ECL Substrate (Bio-Rad Laboratories, Inc.) and were analyzed using ImageJ software (version 1.54; National Institutes of Health).

*Transfection and siRNA knockdown assays*. HepG2 cells were seeded at a density of ~$2x10^5$ cells/well in 6-well plates and transfected with RAB7A small interfering (si)RNAs (si-RAB7A-1, si-RAB7A-2 and si-RAB7A-3) or NC siRNA using Lipofectamine 3000. The final concentration of siRNAs in each well was 50 nM, and transfection was performed at 37˚C for 48 h according to the manufacturer's instructions. After 48 h, transfection efficiency was confirmed using RT-qPCR and western blotting. The siRNA with the highest knockdown efficiency was selected for subsequent experiments and termed si-RAB7A. The siRNA sequences are listed in Table II.

*Dual-luciferase reporter assay*. The 3'-UTR fragment of RAB7A containing the putative miR-448 binding site (wild-type; WT) and the corresponding mutant (MUT) were cloned into the pmirGLO dual-luciferase reporter vector (Promega Corporation). HepG2 cells were co-transfected with pmirGLO constructs and either miR-448 mimics or mimics NC, as aforementioned, using Lipofectamine 3000. After 48 h, luciferase activity was measured using the Dual-Luciferase Reporter Assay System (Promega Corporation) and normalized against *Renilla* luciferase activity.

*Cell viability and proliferation assays*. HepG2 cell viability and proliferation were assessed using CCK-8 (Dojindo Laboratories, Inc.) and EdU incorporation assays (Beyotime Biotechnology). For CCK-8, absorbance was measured at 450 nm at the indicated time points (0, 24, 48, 72 and 96 h). For the EdU assay, cells were incubated with EdU at a final concentration of 10 $\mu$M at 37˚C for 2 h. Cells were then fixed with 4% paraformaldehyde at 25˚C for 15 min and permeabilized with PBS containing 0.3% Triton X-100 at 25˚C for 15 min. EdU staining was performed using the Click reaction cocktail at 25˚C for 30 min in the dark, and nuclei were counterstained with DAPI at 25˚C for 3 min, followed by three washes with PBS (5 min each). $EdU^+$ cells were observed and counted under a fluorescence microscope

Table II. Sequences of siRNAs used for RAB7A knockdown.

| siRNA | Sequence, 5'-3' |
|---|---|
| siRNA NC | S: UUCUCCGAACGUGUCACGUTT |
| | AS: ACGUGACACGUUCGGAGAATT |
| RAB7A siRNA-1 | S: CACAAUAGGAGCUGACUUUTT |
| | AS: AAAGUCAGCUCCUAUUGUGTT |
| RAB7A siRNA-2 | S: UUAUCAUCCUGGGAGAUUCTT |
| | AS: GAAUCUCCCAGGAUGAUAATT |
| RAB7A siRNA-3 | S: CAGUAUGUGAAUAAGAAAUTT |
| | AS: AUUUCUUAUUCACAUACUGTT |

AS, antisense; NC, negative control; RAB7A, Ras-related protein Rab-7a; S, sense; siRNA, small interfering RNA.

(Olympus Corporation) according to the manufacturer's instructions.

*Cell migration and invasion assays*. Migration and invasion were evaluated using 24-well Transwell chambers (pore size, 8 $\mu$m; Corning, Inc.) coated with or without Matrigel (BD Biosciences), respectively. For the invasion assay, Matrigel (BD Biosciences) was thawed at 4˚C overnight and diluted on ice, and 50 $\mu$l was added to the upper chamber and allowed to polymerize at 37˚C for 30 min. Cells were harvested and resuspended in serum-free medium, and $1x10^5$ cells in 200 $\mu$l were seeded into the upper chamber per well, whereas the lower chamber was filled with 800 $\mu$l DMEM containing 10% FBS. The chambers were then incubated at 37˚C with 5% $CO_2$ for 48 h, after which, the Transwell chambers were washed with PBS, fixed with 4% paraformaldehyde for 20 min at 25˚C and stained with 0.5% crystal violet for 5 min at 25˚C. Images of the cells were then captured and the cells were counted under a fluorescence microscope (Olympus Corporation) at x200 magnification.

*Measurement of glycolysis-related metabolites*. HepG2 cells were homogenized in PBS, followed by centrifugation at 10,000 x g for 10 min at 4˚C. The supernatants were then collected, kept on ice and subsequently used for lactate measurement with an L-lactate assay kit (cat. no. A019-2-1; Nanjing Jiancheng Bioengineering Institute) according to the manufacturer's protocol. Intracellular ATP levels were determined using an ATP assay kit (cat. no. S0026; Beyotime Biotechnology) according to the manufacturer's protocol. Glucose uptake was assessed using a fluorescent glucose analog [2-N-(7-nitrobenz-2-oxa-1,3-diazol-4-yl)amino-2-deoxy-D-glucose (2-NBDG); Invitrogen; Thermo Fisher Scientific, Inc.]. Cells were incubated with 2.5 $\mu$g/ml 2-NBDG for 30 min at 37˚C, washed with PBS and analyzed using a NovoCyte flow cytometer (Agilent Technologies, Inc.). Data were processed using NovoExpress software (version 1.5.0; Agilent Technologies, Inc.).

*Measurement of extracellular acidification rate (ECAR)*. The ECAR, as an indicator of glycolytic activity, was measured using a Seahorse XF8 extracellular flux analyzer (Agilent Technologies, Inc.). Briefly, HepG2 cells from the different treatment groups were seeded into XF8 cell culture microplates at a density of $1x10^4$ cells/well and allowed to adhere for 12 h. The culture medium was then replaced with Seahorse XF assay medium according to the manufacturer's instructions, and cells were incubated at 37˚C in a non-$CO_2$ incubator for 60 min to allow equilibration. After baseline measurements were recorded, glucose (10 mM), oligomycin (1 $\mu$M) and 2-deoxy-D-glucose (50 mM) were sequentially injected at the indicated time points by the analyzer, and ECAR was continuously monitored. ECAR data were analyzed using Wave software (version 2.6; Agilent Technologies, Inc.) and used to evaluate glycolytic function.

*Rescue experiment*. To validate that RAB7A mediates the effects of miR-448, HepG2 cells were seeded to reach 70-80% confluence and transfected with a RAB7A overexpression (OE) plasmid (RAB7A OE) or the corresponding empty vector based on the pcDNA3.1 backbone (Changsha Zeqiong Biotechnology Co., Ltd.) using Lipofectamine 3000 according to the manufacturer's instructions at 37˚C. After 24 h of transfection, cells were treated with EXO-miR-448 (25 $\mu$g/ml) at 37˚C. After a further 48 h, cell proliferation, migration, invasion and glycolytic activity were re-assessed as described in the aforementioned methods.

*Bioinformatics analysis*. RAB7A expression in HCC tissues compared with that in normal tissues was analyzed using The Cancer Genome Atlas (TCGA)-Liver Hepatocellular Carcinoma dataset (https://portal.gdc.cancer.gov/). RNA-seq TPM expression data from a total of 424 tumor samples and 50 adjacent normal tissue samples were assessed. Among these samples, 50 normal samples were paired with their corresponding tumor samples, whereas the remaining tumor samples were unpaired. Potential downstream target genes of miR-448, as well as the predicted miR-448 binding site within the 3'-UTR of RAB7A, were identified using the TargetScanHuman database (version 8.0; https://www.targetscan.org). Genes with high context $^{++}$ scores were selected for further analysis.

*Statistical analysis*. Statistical analyses were performed using GraphPad Prism software (version 9.0; Dotmatics). All data are presented as the mean ± SD from ≥3 independent experiments. For paired data, a paired Student's t-test was used. Unpaired Student's t-test or one-way ANOVA followed by Tukey's post hoc test was used for comparison among groups. $P<0.05$ was considered to indicate a statistically significant difference.

## Results

*miR-448 expression is downregulated in liver cancer cells and enriched in exosomes*. RT-qPCR analysis revealed that miR-448 expression was significantly downregulated in liver cancer cell lines (HepG2, Hep3B and SK-HEP-1) compared with in normal THLE-2 liver cells (Fig. 1A). Subsequent experiments involving RNase A treatment of the supernatant of HepG2 cells revealed no significant alteration in miR-448 expression levels; however, treatment with both RNase A and Triton X-100 resulted in a significant reduction of miR-448 levels (Fig. 1B). These findings indicated that miR-448 was

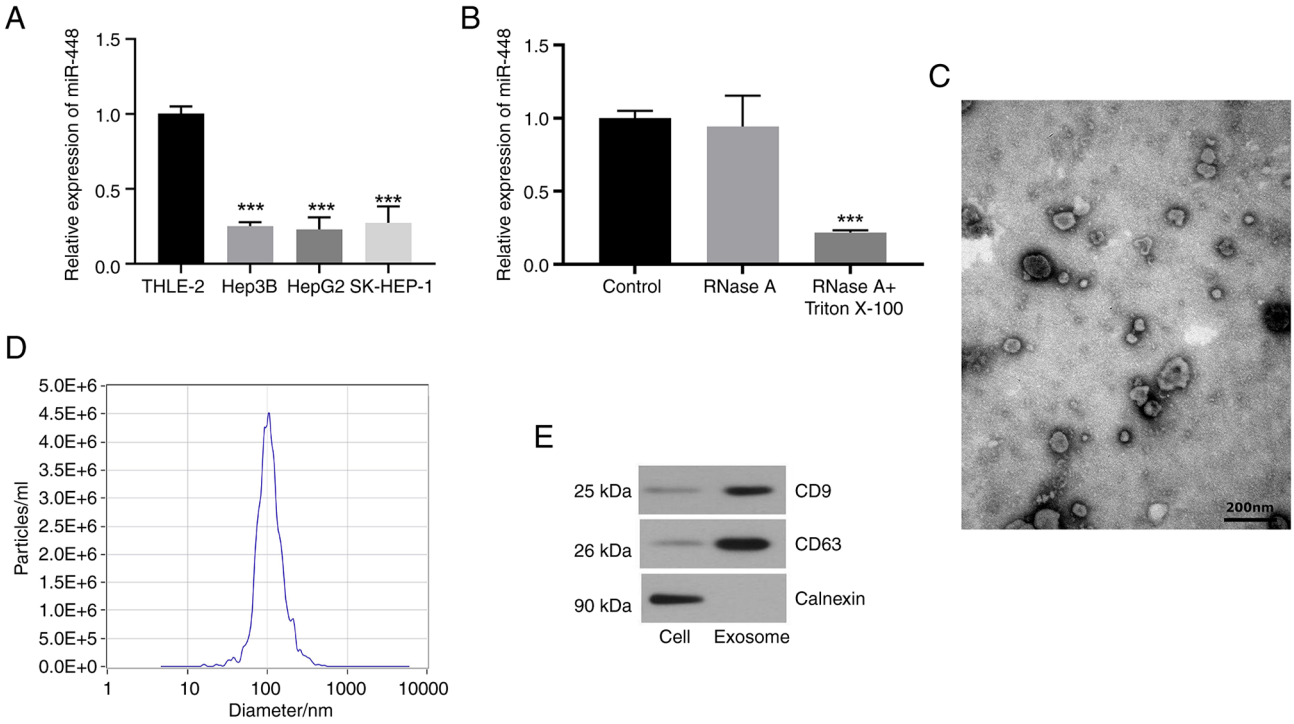


Figure 1. miR-448 expression in liver cancer cell lines and exosome characterization. (A) Relative expression levels of miR-448 in liver cancer cell lines (HepG2, Hep3B and SK-HEP-1) and the normal liver cell line THLE-2, assessed using reverse transcription-quantitative PCR. ***P<0.001 vs. THLE-2. (B) Relative expression levels of miR-448 in exosomes treated with RNase A or RNase A + Triton X-100. ***P<0.001 vs. control. (C) Transmission electron microscopy image of exosomes isolated from HepG2 cells (scale bar, 200 nm). (D) Size distribution of HepG2 derived exosomes determined by nanoparticle tracking analysis, with a peak diameter of ~104 nm. (E) Western blotting of exosome markers (CD9 and CD63) in HepG2 cell lysates and exosomes, with calnexin as a negative control. miR, microRNA.

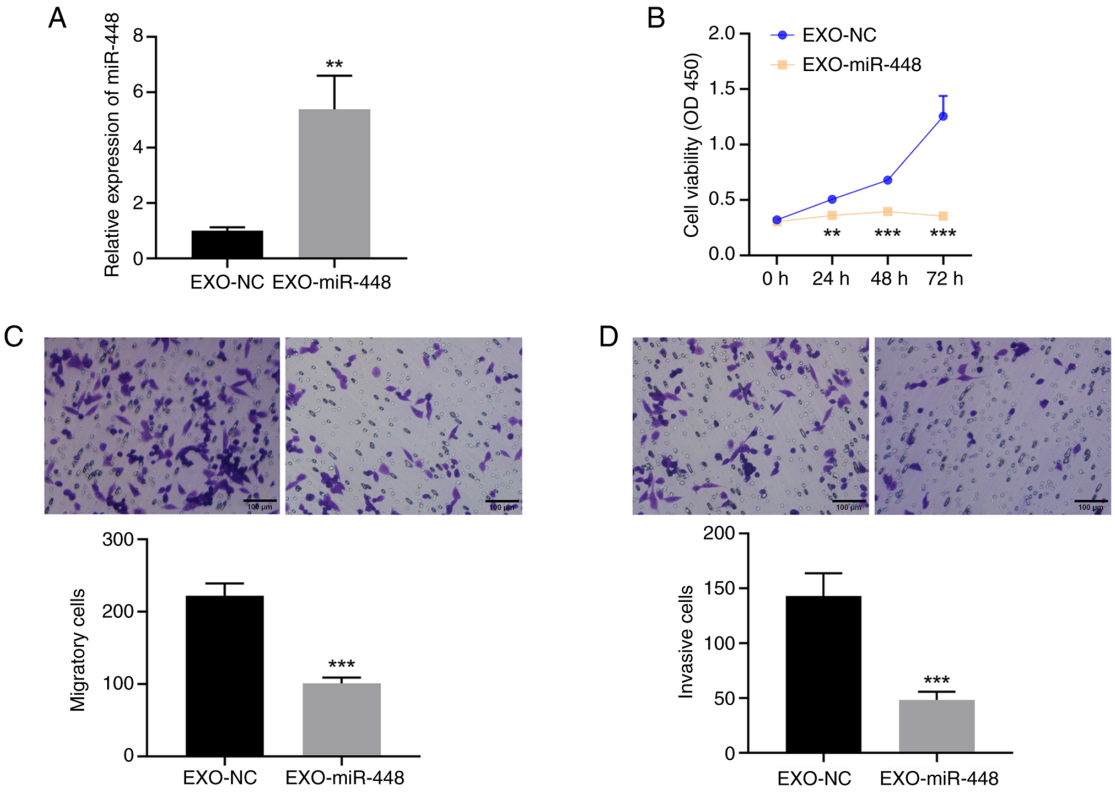


Figure 2. EXO-miR-448 inhibits liver cancer cell proliferation, migration and invasion. (A) Relative expression levels of miR-448 in exosomes derived from HepG2 cells transfected with miR-448 mimics or mimics NC, assessed using reverse transcription-quantitative PCR. **P<0.01 vs. EXO-NC. (B) Cell viability assessed using the Cell Counting Kit-8 assay. **P<0.01 and ***P<0.001 vs. EXO-NC. (C) Migration evaluated using the Transwell migration assays (scale bar, 100 $\mu$m). ***P<0.001 vs. EXO-NC. (D) Invasion assessed using the Transwell invasion assays (scale bar, 100 $\mu$m). ***P<0.001 vs. EXO-NC. miR, microRNA; NC, negative control; EXO, exosomal.

A

| Target gene | Representative transcript ENST0000... | Gene name | Number of 3P-seq tags supporting UTR + 5 | Link to sites in UTRs | Conserved sites | | | | Poorly conserved sites | | | | 6mer sites | Representative miRNA | Predicted occupancy | | | Cumulative weighted context++ score | Total context++ score |
|---|---|---|---|---|---|---|---|---|---|---|---|---|---|---|---|---|---|---|---|
| | | | | | total | 8mer | 7mer-m8 | 7mer-A1 | total | 8mer | 7mer-m8 | 7mer-A1 | | | mod miRNA | high miRNA | trans-fected miRNA | | |
| TMSB4X | 0451311.2 | thymosin beta 4, X-linked | 5 | Sites in UTR | 1 | 1 | 0 | 0 | 1 | 0 | 1 | 0 | 0 | hsa-miR-448 | 0.0503 | 0.3074 | 1.0848 | -1.03 | -1.03 |
| VASH2 | 0366968.4 | vasohibin 2 | 70 | Sites in UTR | 3 | 3 | 0 | 0 | 1 | 0 | 1 | 0 | 0 | hsa-miR-448 | 0.0911 | 0.5854 | 2.2679 | -0.77 | -0.81 |
| SGPP1 | 0247225.6 | sphingosine-1-phosphate phosphatase 1 | 1340 | Sites in UTR | 1 | 1 | 0 | 0 | 1 | 1 | 0 | 0 | 0 | hsa-miR-448 | 0.1134 | 0.6097 | 1.5639 | -0.68 | -0.68 |
| MPC1 | 0360961.6 | mitochondrial pyruvate carrier 1 | 2761 | Sites in UTR | 1 | 1 | 0 | 0 | 0 | 0 | 0 | 0 | 0 | hsa-miR-448 | 0.0548 | 0.2999 | 0.7599 | -0.59 | -0.59 |
| RAB7A | 0265062.3 | RAB7A, member RAS oncogene family | 7894 | Sites in UTR | 1 | 1 | 0 | 0 | 0 | 0 | 0 | 0 | 0 | hsa-miR-448 | 0.0142 | 0.0959 | 0.4393 | -0.48 | -0.48 |

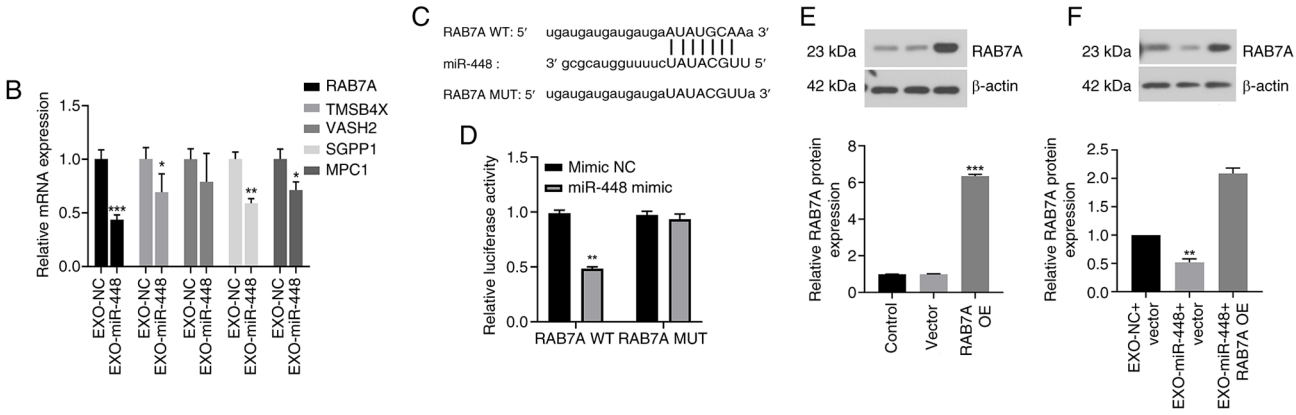


Figure 3. RAB7A as a direct downstream target of miR-448 in liver cancer. (A) Bioinformatics analysis predicted potential downstream targets of miR-448, including RAB7A, TMSB4X, VASH2, SGPP1 and MPC1. (B) Relative mRNA expression levels of candidate targets in HepG2 cells treated with EXO-miR-448 or EXO-NC, assessed using reverse transcription-quantitative PCR. $^{*}$P<0.05, $^{**}$P<0.01 and $^{***}$P<0.001 vs. EXO-NC. (C) Predicted binding sites of miR-448 in the 3'-UTR of RAB7A (WT and MUT). (D) Dual-luciferase reporter assay validating the interaction between miR-448 and RAB7A. $^{**}$P<0.01 vs. mimic NC. (E) Western blotting showing markedly increased RAB7A protein levels in HepG2 cells transfected with the RAB7A OE construct alone. $^{***}$P<0.001 vs. vector. (F) Western blotting showing reduced RAB7A protein levels in HepG2 cells after EXO-miR-448 treatment. $^{**}$P<0.01 vs. EXO-NC + vector. EXO, exosomal; miR, microRNA; MPC1, mitochondrial pyruvate carrier 1; MUT, mutant; NC, negative control; OE, overexpression; RAB7A, Ras-related protein Rab-7a; SGPP1, sphingosine-1-phosphate phosphatase 1; TMSB4X, thymosin β 4 X-linked; VASH2, vasohibin 2; WT, wild-type*s*.

predominantly contained within exosomes, rather than being directly released into the extracellular milieu. Furthermore, exosomes were isolated from the culture medium of HepG2 cells and characterized by TEM and NTA, confirming their typical cup-shaped morphology and a median particle size of ~104 nm, consistent with the expected range for exosomes (Fig. 1C and D). Western blotting demonstrated successful exosome isolation by detecting the exosomal markers CD63 and CD9, with calnexin serving as a negative control (Fig. 1E). These results suggested that miR-448 is not only downregulated in liver cancer cells but also exists in exosomes, potentially serving a role in cell-to-cell communication within the tumor microenvironment.

*EXO-miR-448 inhibits liver cancer cell proliferation, migration and invasion*. To explore the functional role of miR-448 in liver cancer, HepG2 cells were transfected with either miR-448 mimics or mimics NC, and exosomes were collected and named EXO-miR-448 and EXO-NC, respectively. The enrichment of miR-448 in exosomes was confirmed by RT-qPCR (Fig. 2A). To evaluate the biological effects of EXO-miR-448, cell viability, migration and invasion were assessed in HepG2 cells treated with EXO-miR-448 or EXO-NC. The CCK-8 assay (Fig. 2B) demonstrated that EXO-miR-448 significantly reduced cell viability compared with EXO-NC. Furthermore, Transwell migration (Fig. 2C) and invasion assays (Fig. 2D) revealed that EXO-miR-448 treatment led to a significant decrease in both migration and invasion of HepG2 cells compared with those in the EXO-NC group. These results suggested that EXO-miR-448 effectively inhibits the proliferation, migration and invasion of liver cancer cells.

*RAB7A is a direct downstream target of EXO-miR-448 in liver cancer cells*. To identify the downstream targets of miR-448, bioinformatics analysis was performed and several potential target genes were predicted, including RAB7A, TMS4BX, VASH2, SGPP1 and MPC1, all of which exhibited relatively high binding scores (Fig. 3A). To further concentrate the candidates, RT-qPCR was performed in liver cancer cells treated with EXO-miR-448 or EXO-NC to evaluate the mRNA expression levels of these predicted targets. Although all five genes showed a modest decrease following EXO-miR-448 treatment, RAB7A demonstrated the most significant downregulation (Fig. 3B). According to previous studies, RAB7A is associated with exosome trafficking, suggesting its potential functional relevance (20,27,28). Based on these findings, RAB7A was selected as the putative target of miR-448 for further investigation. The predicted binding site of miR-448 on the 3'-UTR of RAB7A is presented in Fig. 3C. A dual-luciferase reporter assay demonstrated that transfection with miR-448 mimics significantly decreased the luciferase activity of the RAB7A WT reporter construct, indicating a direct interaction between miR-448 and RAB7A (Fig. 3D). To confirm the efficiency of RAB7A OE, western blot analysis was performed in cells transfected with the RAB7A OE construct alone. The results demonstrated a significant increase in RAB7A protein levels compared with those in the vector group (Fig. 3E), confirming successful transfection. Furthermore, treatment with EXO-miR-448

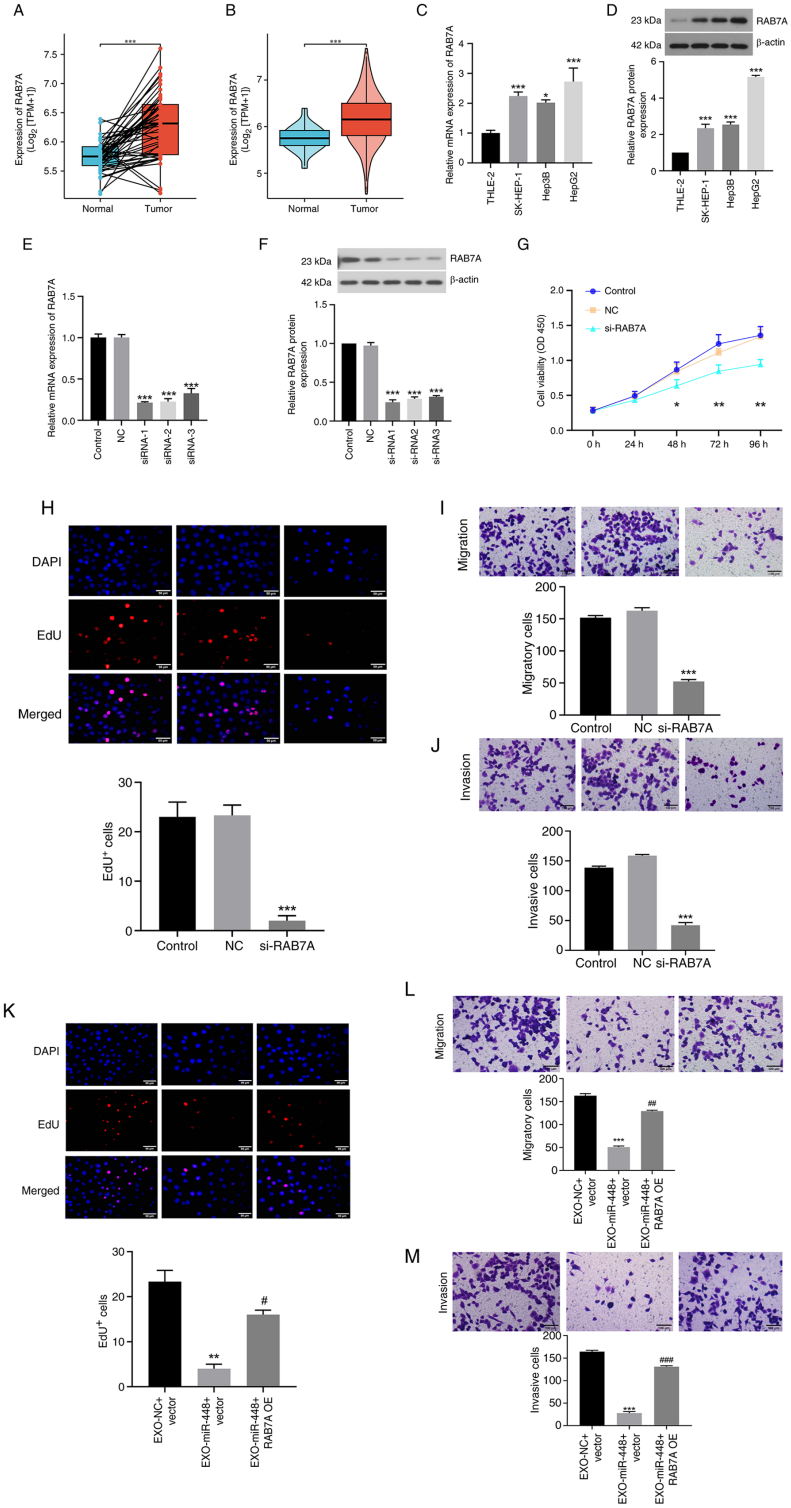


Figure 4. EXO-miR-448 inhibits liver cancer cell proliferation, migration and invasion by targeting RAB7A. (A) Paired comparison of RAB7A expression between HCC tumor tissues and their matched adjacent normal tissues (n=50 pairs). ***P<0.001. (B) Unpaired comparison of all HCC tumor samples (n=424) vs. normal liver tissues (n=50). ***P<0.001. (C) RAB7A mRNA expression in normal liver cells (THLE-2) and liver cancer cell lines (HepG2, Hep3B and SK-HEP-1). *P<0.05 and ***P<0.001 vs. THLE-2. (D) RAB7A protein expression in normal liver cells (THLE-2) and liver cancer cell lines (HepG2, Hep3B and SK-HEP-1). ***P<0.001 vs. THLE-2. (E) Validation of RAB7A knockdown efficiency in HepG2 cells using reverse transcription-quantitative PCR. ***P<0.001 vs. NC. (F) Validation of RAB7A knockdown efficiency in HepG2 cells using western blotting. ***P<0.001 vs. NC. (G) Cell Counting Kit-8 assay showing reduced proliferation of HepG2 cells after RAB7A knockdown. *P<0.05 and **P<0.01 vs. NC. (H) EdU assay showing reduced proliferation of HepG2 cells after RAB7A knockdown (scale bar, 50 $\mu$m). ***P<0.001 vs. NC. (I) Transwell migration assay showing suppressed migratory ability of HepG2 cells following RAB7A knockdown (scale bar, 100 $\mu$m). ***P<0.001 vs. NC. (J) Transwell invasion assay showing suppressed invasive ability of HepG2 cells following RAB7A knockdown (scale bar, 100 $\mu$m). ***P<0.001 vs. NC. (K) Rescue experiment showing that RAB7A OE reverses the inhibitory effect of EXO-miR-448 on HepG2 cell proliferation. scale bar, 50 $\mu$m. **P<0.01 vs. EXO-NC + vector; #P<0.05 vs. EXO-miR-448 + vector. (L) Rescue experiment showing that RAB7A OE reverses the inhibitory effect of EXO-miR-448 on HepG2 cell migration. Scale bar, 100 $\mu$m. ***P<0.001 vs. EXO-NC + vector; ##P<0.01 vs. EXO-miR-448 + vector. (M) Rescue experiment showing that RAB7A OE reverses the inhibitory effect of EXO-miR-448 on HepG2 cell invasion. Scale bar, 100 $\mu$m. ***P<0.001 vs. EXO-NC + vector; ###P<0.001 vs. EXO-miR-448 + vector. EXO, exosomal; HCC, hepatocellular carcinoma; miR, microRNA; NC, negative control; OE, overexpression; RAB7A, Ras-related protein Rab-7a; siRNA, small interfering RNA; TPM, transcripts per million.

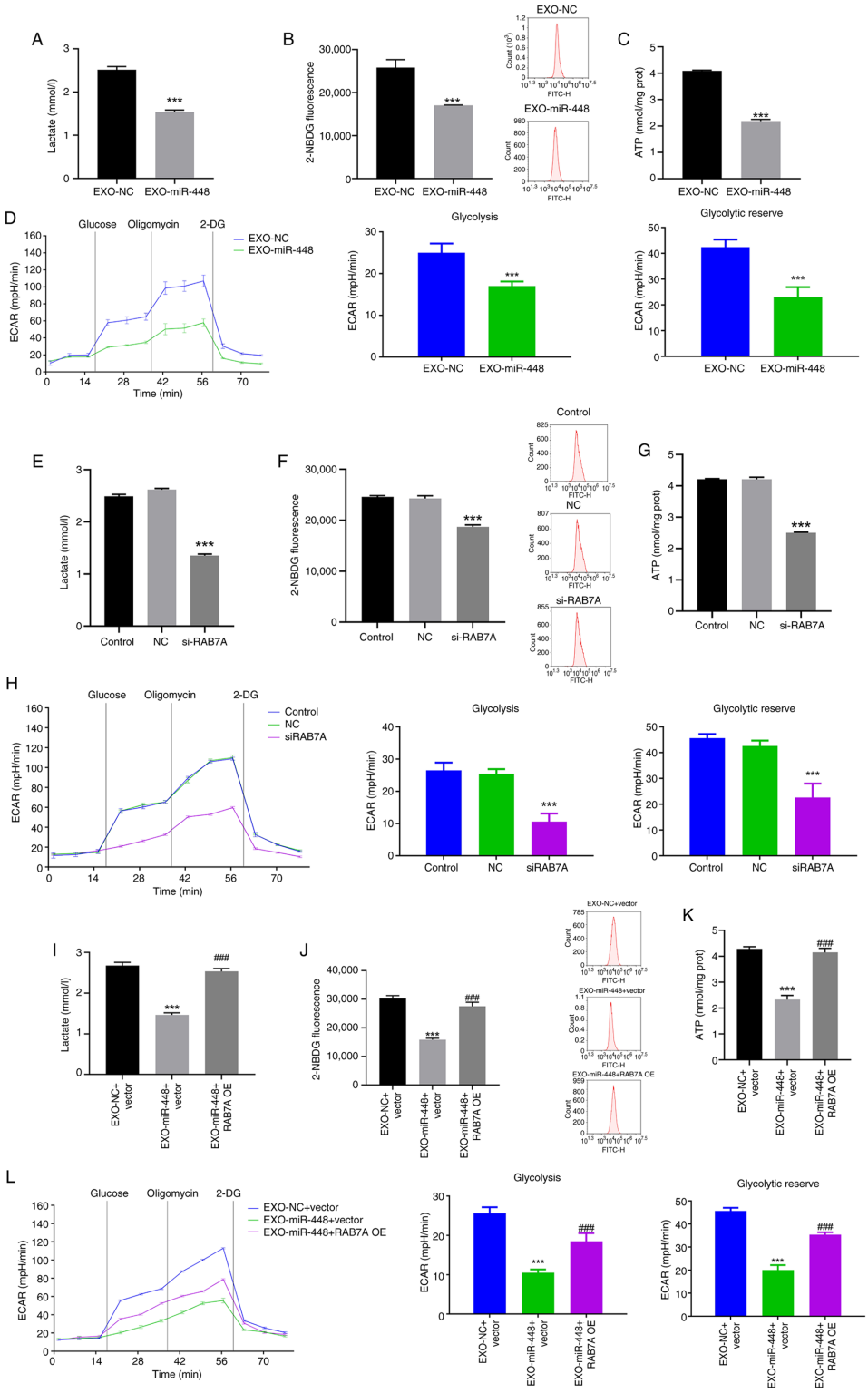


Figure 5. EXO-miR-448 suppresses liver cancer progression by targeting RAB7A to inhibit glycolysis. (A) Lactate production in HepG2 cells treated with EXO-miR-448 or EXO-NC, determined by a colorimetric assay. ***P<0.001 vs. EXO-NC. (B) Glucose uptake in HepG2 cells treated with EXO-miR-448 or EXO-NC, assessed using the 2-NBDG assay. ***P<0.001 vs. EXO-NC. (C) Intracellular ATP levels in HepG2 cells treated with EXO-miR-448 or EXO-NC, determined using an ATP assay kit. ***P<0.001 vs. EXO-NC. (D) ECAR in HepG2 cells treated with EXO-miR-448 or EXO-NC, measured using a Seahorse XF Analyzer. ***P<0.001 vs. EXO-NC. (E) Lactate production in HepG2 cells transfected with si-RAB7A or control siRNA. ***P<0.001 vs. NC. (F) Glucose uptake in HepG2 cells transfected with si-RAB7A or control siRNA. ***P<0.001 vs. NC. (G) Intracellular ATP levels in HepG2 cells transfected with si-RAB7A or control siRNA. ***P<0.001 vs. NC. (H) ECAR in HepG2 cells transfected with si-RAB7A or control siRNA. ***P<0.001 vs. NC. (I) Lactate production in HepG2 cells following EXO-miR-448 treatment with or without RAB7A OE. ***P<0.001 vs. EXO-NC + vector; ###P<0.001 vs. EXO-miR-448 + vector. (J) Glucose uptake in HepG2 cells following EXO-miR-448 treatment with or without RAB7A OE. ***P<0.001 vs. EXO-NC + vector; ###P<0.001 vs. EXO-miR-448 + vector. (K) ATP levels in HepG2 cells following EXO-miR-448 treatment with or without RAB7A OE. ***P<0.001 vs. EXO-NC + vector; ###P<0.001 vs. EXO-miR-448 + vector. (L) ECAR analysis showing glycolytic activity in HepG2 cells following EXO-miR-448 treatment with or without RAB7A OE. ***P<0.001 vs. EXO-NC + vector; ###P<0.001 vs. EXO-miR-448 + vector. miR, microRNA; NC, negative control; ECAR, extracellular acidification rate; si, small interfering RNA; RAB7A, Ras-related protein Rab-7a; NBDG, N-(7-Nitrobenz-2-oxa-1,3-diazol-4-yl)amino-2-deoxy-D-glucose; EXO, exosomal; OE, overexpression; 2-DG, 2-deoxy-D-glucose.

suppressed RAB7A protein expression compared with that in the EXO-NC + vector group (Fig. 3F).

*EXO-miR-448 inhibits liver cancer cell proliferation, migration and invasion by targeting RAB7A*. To further assess the functional role of EXO-miR-448 in liver cancer, its downstream target gene RAB7A was analyzed. Data from TCGA indicated that RAB7A expression was significantly higher in HCC tissues compared with that in normal liver tissues, consistent with the present hypothesis that RAB7A serves a key role in liver cancer progression (Fig. 4A and B). Furthermore, western blotting and RT-qPCR analysis demonstrated that RAB7A expression was significantly upregulated in different liver cancer cells compared with in THLE-2 normal liver cells (Fig. 4C and D). To assess this, RAB7A expression was silenced in liver cancer cells using siRNA targeting RAB7A, and successful knockdown was confirmed using RT-qPCR and western blotting (Fig. 4E and F). Subsequently, the biological effects of RAB7A silencing on liver cancer cells were evaluated. The results revealed that RAB7A knockdown significantly reduced cell proliferation, migration and invasion, as assessed using CCK-8, EdU and Transwell migration and invasion assays, respectively (Fig. 4G-J).

To further explore the impact of EXO-miR-448 on RAB7A-regulated cell behavior, RAB7A was overexpressed in liver cancer cells and the results demonstrated that RAB7A OE rescued the inhibitory effects of EXO-miR-448 on cell proliferation, migration and invasion (Fig. 4K-M). These findings suggested that EXO-miR-448 may suppress liver cancer cell proliferation, migration and invasion by directly targeting RAB7A.

*EXO-miR-448 inhibits glycolysis in liver cancer cells by targeting RAB7A*. To further investigate the mechanism through which EXO-miR-448 affects liver cancer progression, the potential role of RAB7A in regulating glycolysis was explored in liver cancer cells. Glycolysis is a key metabolic pathway that is often upregulated in cancer cells, including liver cancer, to support rapid cell proliferation and metastasis (29,30). To evaluate the effect of EXO-miR-448 on glycolysis in liver cancer cells, HepG2 cells were treated with EXO-miR-448. Glycolysis-associated indicators, including lactate production, glucose uptake and ATP levels, were significantly decreased following EXO-miR-448 treatment (Fig. 5A-C). Furthermore, ECAR, an indicator of glycolytic activity and capacity, was markedly reduced upon EXO-miR-448 exposure (Fig. 5D), further supporting the inhibitory effect of EXO-miR-448 on glycolysis in liver cancer cells. Furthermore, silencing RAB7A expression using siRNA resulted in a similar decrease in glycolytic activity, including significantly reduced lactate production, ATP levels, glucose uptake and ECAR, suggesting that RAB7A is involved in the regulation of glycolysis (Fig. 5E-H). Notably, RAB7A OE reversed the inhibitory effects of EXO-miR-448 on glycolysis, as demonstrated by the significant restoration of lactate production, glucose uptake, ATP levels and ECAR (Fig. 5I-L). Overall, the findings indicated that EXO-miR-448 may regulate glycolysis in liver cancer cells through the direct targeting of RAB7A and this mechanism may contribute to the antitumor effects of miR-448 in liver cancer.

## Discussion

Liver cancer remains one of the most aggressive malignancies. As HCC accounts for 75-85% of primary liver cancer cases, its clinical characteristics largely define the behavior of liver cancer. Notably, the 5-year recurrence rate of HCC after curative resection reaches 40-70%, and long-term survival remains poor, underscoring its high recurrence, metastatic potential and resistance to therapy (31-33). Despite advancements in targeted therapies, prognosis remains poor due to the complexity of its pathogenesis and the lack of effective early detection methods (34,35). Altered metabolism, particularly the upregulation of glycolysis (the Warburg effect), is a hallmark of cancer cells and enables them to meet the bioenergetic and biosynthetic demands of rapid proliferation and metastasis, a feature particularly prominent in liver cancer (36). The aim of the present study was to assess the role of EXO-miR-448 in liver cancer progression, focusing on its potential to target RAB7A and regulate glycolysis.

The results of the present study demonstrated that miR-448 was significantly downregulated in liver cancer cell lines compared with in normal liver cells, consistent with previous studies demonstrating reduced miR-448 expression in HCC tissues and its association with hepatocarcinogenesis (9,37). miRNAs can be actively exported via extracellular vesicles, with exosomes serving as predominant carriers for intercellular transfer of bioactive molecules (38). Aberrant expression levels of exosomal miRNAs have been implicated in multiple malignancies, including lung, breast, colorectal, liver, gastric and pancreatic cancer, where they regulate key tumor-associated processes such as proliferation, angiogenesis, metastasis and chemoresistance (39). The present study revealed that miR-448 was markedly packaged into exosomes derived from HepG2 cells. Functionally, miR-448 has been recognized as a tumor suppressor in several cancer types (40,41), including non-small-cell lung cancer, where it targets sirtuin 1 to inhibit proliferation, migration and epithelial-mesenchymal transition (42). Consistently, the results of the present study indicated that EXO-miR-448 may suppress the proliferation, migration and invasion of liver cancer cells.

A key finding of the present study was that miR-448 targets RAB7A, a small GTPase involved in endosomal maturation, autophagy and intracellular trafficking. Beyond its role in vesicular trafficking and autophagy, RAB7A has been reported to promote tumor metastasis through multiple mechanisms in different malignancies. In HCC, RAB7A OE activates the PI3K/AKT signaling pathway and induces epithelial-mesenchymal transition, thereby enhancing migration and invasion (43). In breast cancer, RAB7A knockdown significantly suppresses proliferation, migration and xenograft tumor growth, confirming its essential contribution to metastatic behavior (44). In melanoma, RAB7A interacts with the endolysosomal channel two pore segment channel 2 to modulate the GSK-3β/β-catenin/microphthalmia-associated transcription factor axis, which drives invasive growth and distant metastasis (45). In colon adenocarcinoma, elevated RAB7A expression has been reported to be associated with increased tumor size, invasion depth, lymph node metastasis and poor overall survival (22). Furthermore, RAB7A upregulation by oncogenic miR-3200 has been reported to promote

telomere remodeling and activate mTOR and autophagy-associated pathways, further supporting its role as a facilitator of malignant progression and dissemination in liver cancer (46). Using dual-luciferase reporter assays, the results of the present study demonstrated that miR-448 can bind to the 3'-UTR of RAB7A, and EXO-miR-448 treatment was further shown to significantly reduce RAB7A mRNA and protein expression. Functional assays further revealed that RAB7A knockdown significantly suppressed cell proliferation, migration and invasion, whereas RAB7A OE rescued the inhibitory effects of EXO-miR-448, indicating that suppression of RAB7A is a key mechanism by which EXO-miR-448 exerts its tumor-suppressive effects in liver cancer.

Notably, the present study revealed that EXO-miR-448 may inhibit glycolysis in liver cancer cells, as demonstrated by significantly reduced lactate production, glucose uptake, ATP levels and ECAR. Consistently, a previous study reported that miR-448 suppresses HCC cell viability and glycolytic activity by directly targeting insulin-like growth factor-1 receptor, leading to decreased glucose uptake, lactate production and ATP generation (47). In the present study, silencing RAB7A produced similar effects, supporting its role as a mediator of EXO-miR-448 driven metabolic suppression. Furthermore, RAB7A OE reversed the inhibitory effects of EXO-miR-448 on glycolysis, restoring lactate production, glucose uptake, ATP levels and ECAR, thereby further demonstrating the functional association between miR-448 and RAB7A in regulating cancer cell metabolism. These findings are further supported by previous studies that demonstrated RAB7A enhances aerobic glycolysis and yes-associated protein 1-driven transcriptional activity to promote HCC growth and metastasis (25,48,49). Furthermore, mechanistic evidence from lipopolysaccharide-activated macrophages indicates that phosphorylation of RAB7A at Ser72 disrupts EGFR endocytosis and sustains glycolytic flux via the pyruvate kinase M2/hypoxia-inducible factor-1α pathway, while disruptions in vesicular trafficking have similarly been reported to alter cellular energy metabolism (50). Notably, RAB7A dysregulation among autophagy-associated genes affected by vacuolar protein sorting 51 deficiency can lead to enhanced glycolysis and impaired oxidative phosphorylation (51). Overall, the ability of RAB7A to coordinate vesicular trafficking, autophagy, nutrient sensing and metabolic stress adaptation may underlie its dual regulatory roles in tumor metabolism and metastatic progression (23,52,53).

Recent studies have further highlighted the intersection of glycolysis, exosome biology and RAB7A in cancer. Lactate accumulation has been reported to drive HCC metastasis by enhancing exosome biogenesis via RAB7A lactylation, thereby associating glycolytic metabolism with RAB7A-mediated vesicular trafficking (54). Furthermore, bone marrow stromal cell-derived exosomal miR-196a-5p has been reported to suppress glycolysis and leukemia progression by targeting 6-phosphofructo-2-kinase/fructose-2,6-biphosphatase 3, underscoring the role of exosome-delivered miRNAs in metabolic regulation (55). The findings of the present study fit within this framework, identifying miR-448 as a novel regulator that inhibits RAB7A-mediated glycolysis via exosomal delivery, thereby attenuating liver cancer.

Nevertheless, the present study had certain limitations. For example, it is limited by its exclusive use of *in vitro* assays. While RAB7A OE rescue experiments strengthen the functional interpretation of the miR-448/RAB7A axis, the lack of *in vivo* validation precludes direct conclusions regarding therapeutic efficacy. Future research should incorporate animal models or patient-derived xenografts to confirm *in vivo* relevance and explore the translational potential of miR-448 mimics or RAB7A inhibitors in liver cancer.

In conclusion, the results of the present study revealed that EXO-miR-448 may inhibit glycolysis and suppress malignant phenotypes in liver cancer cells by directly targeting RAB7A. These findings provide novel mechanistic insights into miRNA-mediated metabolic regulation in liver cancer and suggest that modulation of the miR-448/RAB7A axis could be a potential therapeutic approach, pending validation in *in vivo* models in the future.

**Acknowledgements**

Not applicable.

**Funding**

The present study was funded by the National Natural Science Foundation of China (grant no. 82260125), the Zhongyuan Thousand Talent Program-Youth Outstanding Talent (grant no. 2018), the Research Program of the Education Department of Henan Province (grant no. 21A320001), the Research Program of the Health Commission of Henan Province (grant no. YXKC2020043) and the Hainan Provincial Natural Science Foundation of China (grant nos. 822QN473, 822MS181 and 823RC591).

**Availability of data and materials**

The data generated in the present study may be requested from the corresponding author.

**Authors' contributions**

YC, ZW, FC and WL contributed to the present study conception and design, prepared materials, collected and analyzed the data. YC and QW wrote the first draft of the manuscript, and QW also participated in data organization and statistical analysis. HW, TZ and MN substantially contributed to the acquisition, analysis and interpretation of experimental data. ZW and WL confirm the authenticity of all the raw data. All authors read and approved the final manuscript.

**Ethics approval and consent to participate**

The use of commercially obtained human cell lines was approved by the Ethics Committee of The Second Affiliated Hospital of Hainan Medical University (Haikou, China) and all procedures were performed in accordance with institutional guidelines.

**Patient consent for publication**

Not applicable.

## Competing interests

The authors declare that they have no competing interests.

## References


1. Sung H, Ferlay J, Siegel RL, Laversanne M, Soerjomataram I, Jemal A and Bray F: Global cancer statistics 2020: GLOBOCAN estimates of incidence and mortality worldwide for 36 cancers in 185 countries. CA Cancer J Clin 71: 209-249, 2021.
2. Marengo A, Rosso C and Bugianesi E: Liver cancer: Connections with obesity, fatty liver, and cirrhosis. Annu Rev Med 67: 103-117, 2016.
3. Hoshida Y, Fuchs BC, Bardeesy N, Baumert TF and Chung RT: Pathogenesis and prevention of hepatitis C virus-induced hepatocellular carcinoma. J Hepatol 61 (Suppl 1): S79-S90, 2014.
4. Alawyia B and Constantinou C: Hepatocellular carcinoma: A narrative review on current knowledge and future prospects. Curr Treat Options Oncol 24: 711-724, 2023.
5. Khameneh SC, Razi S, Lashanizadegan R, Akbari S, Sayaf M, Haghani K and Bakhtiyari S: MicroRNA-mediated metabolic regulation of immune cells in cancer: An updated review. Front Immunol 15: 1424909, 2024.
6. He L and Hannon GJ: MicroRNAs: Small RNAs with a big role in gene regulation. Nat Rev Genet 5: 522-531, 2004.
7. Bartel DP: MicroRNAs: Target recognition and regulatory functions. Cell 136: 215-233, 2009.
8. Xu X, Li Y, Zhang R, Chen X, Shen J, Yuan M, Chen Y, Chen M, Liu S, Wu J and Sun Q: Jianpi Yangzheng decoction suppresses gastric cancer progression via modulating the miR-448/CLDN18.2 mediated YAP/TAZ signaling. J Ethnopharmacol 311: 116450, 2023.
9. Zhu H, Zhou X, Ma C, Chang H, Li H, Liu F and Lu J: Low expression of miR-448 induces EMT and promotes invasion by regulating ROCK2 in hepatocellular carcinoma. Cell Physiol Biochem 36: 487-498, 2015.
10. Lin Z, Zhu Y and Liu Y: The role of miR-448 in cancer progression and its potential therapeutic applications. J Cancer Res Clin Oncol 143: 679-687, 2017.
11. Jiang X, Zhou Y, Sun AJ and Xue JL: NEAT1 contributes to breast cancer progression through modulating miR-448 and ZEB1. J Cell Physiol 233: 8558-8566, 2018.
12. Zhou Y, Lin F, Wan T, Chen A, Wang H, Jiang B, Zhao W, Liao S, Wang S, Li G, *et al*: ZEB1 enhances Warburg effect to facilitate tumorigenesis and metastasis of HCC by transcriptionally activating PFKM. Theranostics 11: 5926-5938, 2021.
13. Zhang J, Ouyang F, Gao A, Zeng T, Li M, Li H, Zhou W, Gao Q, Tang X, Zhang Q, *et al*: ESM1 enhances fatty acid synthesis and vascular mimicry in ovarian cancer by utilizing the PKM2-dependent Warburg effect within the hypoxic tumor microenvironment. Mol Cancer 23: 94, 2024.
14. Jing Z, Liu Q, He X, Jia Z, Xu Z, Yang B and Liu P: NCAPD3 enhances Warburg effect through c-myc and E2F1 and promotes the occurrence and progression of colorectal cancer. J Exp Clin Cancer Res 41: 198, 2022.
15. Peng L, Zhao Y, Tan J, Hou J, Jin X, Liu DX, Huang B and Lu J: PRMT1 promotes Warburg effect by regulating the PKM2/PKM1 ratio in non-small cell lung cancer. Cell Death Dis 15: 504, 2024.
16. Paul S, Ghosh S and Kumar S: Tumor glycolysis, an essential sweet tooth of tumor cells. Semin Cancer Biol 86: 1216-1230, 2022.
17. Lan F, Qin Q, Yu H and Yue X: Effect of glycolysis inhibition by miR-448 on glioma radiosensitivity. J Neurosurg 132: 1456-1464, 2019.
18. Luce A, Lombardi A, Ferri C, Zappavigna S, Tathode MS, Miles AK, Boocock DJ, Vadakekolathu J, Bocchetti M, Alfano R, *et al*: A proteomic approach reveals that miR-423-5p modulates glucidic and amino acid metabolism in prostate cancer cells. Int J Mol Sci 24: 617, 2022.
19. Chu M, Zhao Y, Feng Y, Zhang H, Liu J, Cheng M, Li L, Shen W, Cao H, Li Q and Min L: MicroRNA-126 participates in lipid metabolism in mammary epithelial cells. Mol Cell Endocrinol 454: 77-86, 2017.
20. Guerra F and Bucci C: Role of the RAB7 protein in tumor progression and cisplatin chemoresistance. Cancers (Basel) 11: 1096, 2019.
21. Ju L, Luo Y, Cui X, Zhang H, Chen L and Yao M: CircGPC3 promotes hepatocellular carcinoma progression and metastasis by sponging miR-578 and regulating RAB7A/PSME3 expression. Sci Rep 14: 7632, 2024.
22. Shan Z, Chen X, Chen H and Zhou X: Investigating the impact of Ras-related protein RAB7A on colon adenocarcinoma behavior and its clinical significance. Biofactors 51: e70006, 2025.
23. Liu Q, Bai Y, Shi X, Guo D, Wang Y, Wang Y, Guo WZ and Zhang S: High RAS-related protein Rab-7a (RAB7A) expression is a poor prognostic factor in pancreatic adenocarcinoma. Sci Rep 12: 17492, 2022.
24. Güleç Taşkıran AE, Hüsnügil HH, Soltani ZE, Oral G, Menemenli NS, Hampel C, Huebner K, Erlenbach-Wuensch K, Sheraj I, Schneider-Stock R, *et al*: Post-transcriptional regulation of Rab7a in lysosomal positioning and drug resistance in nutrient-limited cancer cells. Traffic 25: e12956, 2024.
25. Zhang JY, Zhu X, Liu Y and Wu X: The prognostic biomarker RAB7A promotes growth and metastasis of liver cancer cells by regulating glycolysis and YAP1 activation. J Cell Biochem 125: e30621, 2024.
26. Livak KJ and Schmittgen TD: Analysis of relative gene expression data using real-time quantitative PCR and the 2(-Delta Delta C(T)) method. Methods 25: 402-408, 2001.
27. Ostrowski M, Carmo NB, Krumeich S, Fanget I, Raposo G, Savina A, Moita CF, Schauer K, Hume AN, Freitas RP, *et al*: Rab27a and Rab27b control different steps of the exosome secretion pathway. Nat Cell Biol 12: 19-30, 1-13, 2010.
28. Mulligan RJ and Winckler B: Regulation of endosomal trafficking by Rab7 and its effectors in neurons: Clues from charcot-marie-tooth 2B disease. Biomolecules 13: 1399, 2023.
29. Hanahan D and Weinberg RA: Hallmarks of cancer: The next generation. Cell 144: 646-674, 2011.
30. Feng J, Li J, Wu L, Yu Q, Ji J, Wu J, Dai W and Guo C: Emerging roles and the regulation of aerobic glycolysis in hepatocellular carcinoma. J Exp Clin Cancer Res 39: 126, 2020.
31. Wen T, Jin C, Facciorusso A, Donadon M, Han HS, Mao Y, Dai C, Cheng S, Zhang B, Peng B, *et al*: Multidisciplinary management of recurrent and metastatic hepatocellular carcinoma after resection: An international expert consensus. Hepatobiliary Surg Nutr 7: 353-371, 2018.
32. Abdelhamed W and El-Kassas M: Hepatocellular carcinoma recurrence: Predictors and management. Liver Res 7: 321-332, 2023.
33. Bray F, Ferlay J, Soerjomataram I, Siegel RL, Torre LA and Jemal A: Global cancer statistics 2018: GLOBOCAN estimates of incidence and mortality worldwide for 36 cancers in 185 countries. CA Cancer J Clin 68: 394-424, 2018.
34. Shin H and Yu SJ: A concise review of updated global guidelines for the management of hepatocellular carcinoma: 2017-2024. J Liver Cancer 25: 19-30, 2025.
35. Llovet JM, Kelley RK, Villanueva A, Singal AG, Pikarsky E, Roayaie S, Lencioni R, Koike K, Zucman-Rossi J and Finn RS: Hepatocellular carcinoma. Nat Rev Dis Primers 7: 6, 2021.
36. Yang F, Hilakivi-Clarke L, Shaha A, Wang Y, Wang X, Deng Y, Lai J and Kang N: Metabolic reprogramming and its clinical implication for liver cancer. Hepatology 78: 1602-1624, 2023.
37. Katayama Y, Maeda M, Miyaguchi K, Nemoto S, Yasen M, Tanaka S, Mizushima H, Fukuoka Y, Arii S and Tanaka H: Identification of pathogenesis-related microRNAs in hepatocellular carcinoma by expression profiling. Oncol Lett 4: 817-823, 2012.
38. Pegtel DM and Gould SJ: Exosomes. Annu Rev Biochem 88: 487-514, 2019.
39. Li B, Cao Y, Sun M and Feng H: Expression, regulation, and function of exosome-derived miRNAs in cancer progression and therapy. FASEB J 35: e21916, 2021.
40. Wu X, Tang H, Liu G, Wang H, Shu J and Sun F: miR-448 suppressed gastric cancer proliferation and invasion by regulating ADAM10. Tumour Biol 37: 10545-10551, 2016.
41. Bamodu OA, Huang WC, Lee WH, Wu A, Wang LS, Hsiao M, Yeh CT and Chao TY: Aberrant KDM5B expression promotes aggressive breast cancer through MALAT1 overexpression and downregulation of hsa-miR-448. BMC Cancer 16: 160, 2016.
42. Qi H, Wang H and Pang D: miR-448 promotes progression of non-small-cell lung cancer via targeting SIRT1. Exp Ther Med 18: 1907-1913, 2019.

43. Liu Y, Ma J, Wang X, Liu P, Cai C, Han Y, Zeng S, Feng Z and Shen H: Lipophagy-related gene RAB7A is involved in immune regulation and malignant progression in hepatocellular carcinoma. Comput Biol Med 158: 106862, 2023.
44. Xie J, Yan Y, Liu F, Kang H, Xu F, Xiao W, Wang H and Wang Y: Knockdown of Rab7a suppresses the proliferation, migration, and xenograft tumor growth of breast cancer cells. Biosci Rep 39: BSR20180480, 2019.
45. Abrahamian C, Tang R, Deutsch R, Ouologuem L, Weiden EM, Kudrina V, Blenninger J, Rilling J, Feldmann C, Kuss S, *et al*: Rab7a is an enhancer of TPC2 activity regulating melanoma progression through modulation of the GSK3β/β-Catenin/MITF-axis. Nat Commun 15: 10008, 2024.
46. Song S, Xie S, Liu X, Li S, Wang L, Jiang X and Lu D: miR-3200 accelerates the growth of liver cancer cells by enhancing Rab7A. Noncoding RNA Res 8: 675-685, 2023.
47. Wang Y, Chen X, Yao N, Gong J, Cao Y, Su X, Feng X and Tao M: MiR-448 suppresses cell proliferation and glycolysis of hepatocellular carcinoma through inhibiting IGF-1R expression. J Gastrointest Oncol 13: 355-367, 2022.
48. Qi C, Zou L, Wang S, Mao X, Hu Y, Shi J, Zhang Z and Wu H: Vps34 inhibits hepatocellular carcinoma invasion by regulating endosome-lysosome trafficking via Rab7-RILP and Rab11. Cancer Res Treat 54: 182-198, 2022.
49. Yang CC, Meng GX, Dong ZR and Li T: Role of Rab GTPases in hepatocellular carcinoma. J Hepatocell Carcinoma 8: 1389-1397, 2021.
50. Zhang X, Chen C, Ling C, Luo S, Xiong Z, Liu X, Liao C, Xie P, Liu Y, Zhang L, *et al*: EGFR tyrosine kinase activity and Rab GTPases coordinate EGFR trafficking to regulate macrophage activation in sepsis. Cell Death Dis 13: 934, 2022.
51. Aygun D and Yücel Yılmaz D: From gene to pathways: Understanding novel Vps51 variant and its cellular consequences. Int J Mol Sci 26: 5709, 2025.
52. Edinger AL, Cinalli RM and Thompson CB: Rab7 prevents growth factor-independent survival by inhibiting cell-autonomous nutrient transporter expression. Dev Cell 5: 571-582, 2003.
53. Deffieu MS, Cesonyte I, Delalande F, Boncompain G, Dorobantu C, Song E, Lucansky V, Hirschler A, Cianferani S, Perez F, *et al*: Rab7-harboring vesicles are carriers of the transferrin receptor through the biosynthetic secretory pathway. Sci Adv 7: eaba7803, 2021.
54. Jiang C, He X, Chen X, Huang J, Liu Y, Zhang J, Chen H, Sui X, Lv X, Zhao X, *et al*: Lactate accumulation drives hepatocellular carcinoma metastasis through facilitating tumor-derived exosome biogenesis by Rab7A lactylation. Cancer Lett 627: 217636, 2025.
55. Fan B, Wang L, Hu T, Zheng L and Wang J: Exosomal miR-196a-5p secreted by bone marrow mesenchymal stem cells inhibits ferroptosis and promotes drug resistance of acute myeloid leukemia. Antioxid Redox Signal 42: 933-953, 2025.